# The role of Plasmonic metal-oxides core-shell nanoparticles on the optical absorption of Perovskite solar cells

**Ihsan Ullah** ( ehsankhan892@gmail.com )
Soochow University, Suzhou, China https://orcid.org/0000-0002-1975-0683
**Hamed Saghaei**
Islamic Azad University
**Said Karim Shah**
Abdul Wali Khan University, Mardan, KhyberPukhtonKhwa

**Research Article**

**Keywords:** Gold nanoparticle, Perovskite solar cell, Surface plasmons, Optical absorption, Core-shell nanoparticle

**Posted Date:** November 10th, 2021

**DOI:** https://doi.org/10.21203/rs.3.rs-887610/v1

# Abstract

Among all the different methods to enhance the optical absorption of photovoltaic devices. The plasmonic effect is one the most prominent and effective ways to capture more incident light and also provide good carrier dynamic management. Here, we systematically introduce spherical gold nanoparticles (Au NPs) with different radii in the absorber layer of perovskite solar cells (PSCs). The overall enhanced optical absorption around 14.20% and 20.02% is achieved for incorporated monolayer and bilayer Au NPs, respectively, in the active layer compared to the pure perovskite layer. Moreover, we employ the metal (Au)-dielectric ($TiO_2$ and $SiO_2$) nanoparticles in the absorber layer. The optical absorption increases as the core-shell size decreases. The optical absorption elevates in both Au@$TiO_2$ core-shell and Au@$SiO_2$ core-shell 17.5% and 3.5%, respectively. These results support superior separation and transfer of charge in the existence of plasmonic NPs. In addition, this study presents a very sophisticated approach in the optical enhancement of PSCs and thus helps to boost the overall photovoltaic device performance.


# 1. Introduction

The photovoltaic effect is the conversion of incident light into useful electricity. Among all solar cell materials, perovskite solar cells (PSCs) is considered one of the most prominent and promised candidate in solar cells industries owing to their excellent properties such as cheaper cost, low-temperature chemical processing and fabrication [1, 2], strong absorption of sunlight [3], higher mobility of carriers and low rate of non-radiative carrier recombination [4]. In addition, flexible PSCs of different colors can be fabricated effectively and advantageous to utilize large and wide wavelength ranges. The important parts of PSCs are transparent conductive oxides (FTO, ITO), electron transport layer (ETL), absorber layer (perovskite), hole transport layer (HTL), and the metal contact [5]. Miyasaka's group presented the first-ever report and replaced dye-sensitized solar cells with perovskite ($Ch_3NH_3PbI_3$) used as liquid sensitizer and achieved power conversion efficiency (PCE) of 3.8%[6]. Kim et al. presented a successful report using perovskite as an active layer, and they also introduced Spiro-MeoTAD as a hole transport layer (HTL) and mesoporous $TiO_2$ as an electron transport layer (ETL). The PCE was achieved 9.7%, almost three times higher than the one presented in the previous report[7]. Moreover, 22.1% certified PCE has been investigated for PSCs and is highly expected to jump over 30%[8]. The optimization of different parameters used in PSCs has become practicable by the rapid efficiency improvements. Each component has its role in improving optical absorption, PCEs, and stability. For instance, the perovskite layer thickness is a dominant factor that extensively affects the absorption of light and the charge separation in HTL and ETL, respectively [9]. The thin layer of perovskite has not the capability to utilize more light, but on the other hand, it provides a good pathway for charge separation. To resolve this hindrance an alternative solution is needed to enhance optical absorption and improve PSCs device performance without increasing the thickness of the perovskite absorber layer. In such circumstances, the surface plasmon resonance effect is one of the best solutions that utilize metal at nanoscale embedded in PSCs; when the incoming light from the sun strikes the metal nanoparticle inside the absorber layer; as a result,

electrons start shining on the surface of metals, such phenomenon of collectively shining of electrons on the surface of metal is called localized surface plasmon resonance (LSPR) and thus enable the solar cells to harvest more light. These LSPR also provide strong electromagnetic field that leads to enhanced scattering cross sections and extinction cross section for larger atoms [10].

The effect of LSPR has extensively been studied in many photovoltaic devices besides PSCs, such as silicon-based solar cells [11], dye-sensitized solar cells (DSSC) [12], and organic solar cells (OSC) [13]. Zhang et al. first investigated the plasmonic effect in PSCs using metal nanoparticles (NPs) and enhanced PCE to 9.5 % as compared to controlled devices (8.4%) [14]. Furasova et al. studied the effect of silicon NPs in PSCs that optimize the PCE up to 18.8% compared to the controlled device without NPs at 17.7% [15]. Batmunkh et al. reported the influence of gold nanostars on mesoporous TiO2 photoanode in PSCs; they observed the PCE increased from 15.19–17.72%. Moreover, enhanced optical absorption and reduced charged recombination were also investigated [16]. Aeineh et al. introduced multifunctional Au@$SiO_2$ core-shell in PSCs and thus improved the device performance because of the plasmonic effect [17]. The Au@$SiO_2$ in PSCs is also capable of improved device stability. The stability is due to the $SiO_2$ coating that acts as a shield and protects Au and the perovskite layer. However, a big gap still exists to wisely utilize the plasmonic effect of nanoparticles with various geometries in PSCs structure. These plasmonic nanoparticles can dramatically change the performance of PSCs in terms of absorption, scattering, efficiency, and stability. Moreover, LSPR caused by these nanoparticles depends on the shape, size, and dielectric function procured by the embedded nanoparticles [18, 19].

In this paper, we performed the optical simulation of embedded Au NPs with different radii (g), Au@$TiO_2$, and Au@$SiO_2$ with different shell thickness ($S_{tk}$) in the absorber layer of PSC in the wavelength range, i.e., 300–800 nm. The plasmonic effect and the corresponding enhancement in the UV-Vis spectrum were systemically observed for each scheme by tailoring the radius (g) of Au NPs and shell thickness ($S_{tk}$). Then we further calculated the bandgap energy for each geometry (Au NPs, Au@$TiO_2$, and Au@$SiO_2$ modified inside the perovskite layer with the help of Tauc's curve. In addition, we finally compared all the results and investigated that the overall optical enhancement in PSC is dedicated to Au@$TiO_2$ as compared to simple Au NPs and Au@$SiO_2$, thus providing a useful track for enhancement and improved stability of PSCs.

# 2. Physical Structure

We first systemically studied the influence of Au NPs, Au@$TiO_2$, and Au@$SiO_2$ on the optical properties of PSCs; we used the finite element method (FEM) in all numerical simulations. Our proposed PSC model is depicted in Fig. 1a. PSC structure normally consists of different functional layers like ITO/$TiO_2$/Perovskite layer/Spiro-OMeTAD/Au. The thickness chosen for all the mentioned parameters were 150nm, 60nm, 250nm, 80, and 60nm, respectively. The refractive index assumed for glass substrate is 1.5. The dielectric function of gold used in the present work is according to the Johnson and Christy model presented in [20]. The complex refractive index of ITO, $TiO_2$, Spiro-OMeTAD and perovskite are

chosen from literature for simulation, respectively [21, 22]. In this simulating model, the entire simulation was performed in a unit cell. To obtain more precise and promised results, we employed tetrahedral meshing for the frequency-domain solver. The structure, as mentioned earlier, is composed of stacked layers obtained from distinct materials, which constitute a sandwich-type configuration. In this work, spherical-shaped plasmonic Au NPs with different sizes were incorporated in $TiO_2$, and $SiO_2$ of various shell thickness ($S_{tk}$) of plasmonic nanoparticles is studied for the perovskite active layer shown in Fig. 1.

An array of equally distributed NPs inside the absorber layer of PSCs is studied. Therefore, symmetry boundary conditions were practiced in the x- and y- axes. The regular two-dimensional patterned structure is shown in Fig. 2 (a, b). To make our model more practical, the background environment is filled with air. The z-axis is kept “open (add space)” for an incoming electromagnetic wave to enable the perovskite layer to absorb the incident light. The simulated model shows that the incident electromagnetic wave propagates in the z-direction while x- and y- directions are dedicated to magnetic and electric fields, respectively. Radiofrequency (RF) module is used by enabling the scattered field formulation to model the optical properties of the full stack proposed device. The standard solar spectrum AM1.5 and irradiance 100 W/$m^2$ is employed in the photovoltaic device. Moreover, the following mathematical equation is used to calculate optical absorption coefficient A(λ).

$$A(\lambda) = 1 - R(\lambda) - T(\lambda); \qquad (1)$$

where lambda (λ), R, and T represent the wavelength, reflection, and transmission of light, respectively. The interaction of electromagnetic wave (EMW) with metal NPs that tend to excite electrons results in further generation of surface plasmon polariton. Maxwell’s equations are used to calculate it mathematically when EMW propagates between metal and dielectric.

# 3. Results And Discussions

Initially, we have studied the influence of Au NP, incorporated in the active layer of PSC, on optical absorption, as shown in Fig. 3a. The size of Au NP was first chosen as 30 nm and then increased to 40 nm and 50 nm, respectively. The results showed that as the Au NPs size increases, the absorption also increases compared to the neat PSC (without Au NPs), as shown in Fig. 3b. This optical absorption enhancement is mainly because of the strong near-field and far-field scattering caused by plasmonic NPs. The enhanced and broadband absorption, i.e., 550–800 nm investigate due to the dielectric properties of Au NP [23]. To further validate our results, we obtained the optical bandgap energy using the Tauc curve [24, 25]. The bandgap energy decreases from 1.69eV (without Au NPs) to 1.61eV, 1.53eV and 1.51eV as the nanoparticles size increased from 30 to 50 nm, respectively as shown in Fig .3c. As a result, the energy required to excite electrons is reduced, so electrons will easily jump from the valence band to the conduction band. Moreover, we further analyzed the optical absorption of the active layer with and without Au NPs in the simulations. Therefore, we calculated the percent amount of absorption enhancement of absorber layer by using Au NPs with various radii, taking the absorption value for the

active layer without plasmonic effect as a reference for comparison. The corresponding enhancement in absorption values (6.2%, 10.92% and 18.32%) for the diameters 30nm, 40nm and 50nm, respectively as shown in Table.1.

Table 1
Comparison of normalized absorption of PSCs with and without Au NP

| Structure | Values of normalized absorption of neat PSC (%) | Values of normalized absorption of PSC with Au NP (%) | Enhancement in normalized absorption (%) |
|---|---|---|---|
| Pure Perovskite | 76.84 | - | - |
| Au NP (g = 30nm) | - | 82.36 | 7.18 |
| Au NP (g = 40nm) | - | 84.87 | 10.92 |
| Au NP (g = 50nm) | - | 87.60 | 14.20 |
| Bilayer NPs (50nm) | - | 91.46 | 20.02 |

In addition, we further explored the influence of bilayer Au NPs placed inside the absorber layer in the z-direction. The size of 50nm (AuNPs) was chosen for the bilayer; this is the extreme size of NPs because there was not enough space to put more NPs in the unit space designed. The enhancement in UV-Vis spectrum for bilayer Au NPs incorporated in the perovskite layer is depicted in Fig. 4a.

The optical absorption spectrum of the bilayer Au NPs embedded perovskite layer is compared with single Au NPs incorporated and without Au NP in the absorber layer. The results showed further enhancement in optical absorption up to 91.46%, as reported in Table 1. The percent increment is also investigated in the case of bilayer Au NPs up to 6% and 14% compared to single NPs embedded in the active layer and pure perovskite, respectively. The Tauc curve is depicted in Fig. 4b. The Tauc curve showed that the decrease in bandgap energy strongly supports our previous results because of the optimization of Au NPs and LSPR effects.

## 4. Effect Of Metal-dielectric Core-shell Thickness On Optical Absorption Of Psc

# 4.1 Effect of Au@$TiO_2$ shell thickness:

In this section, we have studied the influence of Au@$TiO_2$ shell thickness ($S_{tk}$) on the optical properties of PSCs. The schematic of Au@$TiO_2$ embedded in the perovskite layer is shown in Fig. 5a. The optical

absorption spectrum, as shown in Fig. 5b suggests that the $S_{tk}$ has a positive effect on the optical performance of PSCs. The broad-spectrum is achieved between 630 and 800 nm as the $S_{tk}$ decreases; at the same time, the shell layer improves the stability of NPs and minimizes the recombination effect by providing safety to avoid unnecessary interaction between NP and absorber layer [26]. Moreover, the converted hot electrons originated from the absorbed photons are linked to the Landau damping, which happens when the phase velocity of electromagnetic approaches that of the plasma particles and possesses superior coupling with each other [27]. When these hot electrons arrive at the perovskite layer, they provide a very sophisticated path to utilize more useful energy around the electromagnetic waves and thus improve the carrier dynamics in the device. In addition, the Tauc curve, as shown in Fig. 5c, also provided information about bandgap and the comparison of different shell $S_{tk}$ used in the simulation, the bandgap energy of PSC without Au@$TiO_2$ is about 1.89eV, with embeded only $TiO_2$ inside the absorber layer is 1.85eV and with Au@$TiO_2$.

The bandgap is reduced to 1.6eV, 1.55eV, and 1.52eV for shell thickness $S_{tk}$=40nm, 30nm, and 20nm, respectively. Moreover, the percentage increase in the UV-Vis spectrum is listed in the Table. 2. The normalized absorption of neat PSC is the same as the embedded only spherical $TiO_2$ NPs while using Au@$TiO_2$ inside the absorber layer; the overall absorbance increased to 9.52%, 15.64%, and 17.23% for different $S_{tk}$ 40nm, 30nm, and 20nm respectively. The enhancement of the UV-Vis spectrum in PSC is because of the transfer of electrons from Au NPs to $TiO_2$ and is also dedicated to the light scattering phenomenon in metallic NP[28, 29].

Table 2
**Comparison of normalized absorption of PSCs with and without Au@ $TiO_2$ core-shell**

| Structure | Values of normalized absorption of neat PSC (%) | Values of normalized absorption of PSC with core-shell (%) | Enhancement in normalized absorption (%) |
|---|---|---|---|
| Pure Perovskite | 76.84 | | |
| Pure $TiO_2$ | 76.84 | - | 0 |
| Au@$TiO_2$ (40nm) | - | 84.26 | 9.52 |
| Au@$TiO_2$ (30nm) | - | 88.84 | 15.64 |
| Au@$TiO_2$ (20nm) | - | 90.02 | 17.23 |

# 4.2 Effect of Au@$SiO_2$ shell thickness

Here we performed the detailed simulations of $Au@SiO_2$ incorporated in the perovskite layer as depicted in Fig. 6a, and their impact on the optical absorption spectrum of PSC. The absorption spectrum for this scheme is shown in Fig. 6a. A very slight increase is observed in the optical spectrum of PSCs with $Au@SiO_{2,}$ which means that the silica shell has no prominent impact on the optical enhancement, or the shell layer has a very small influence on the optical properties due to the dielectric properties of surrounding NP after coating. However, dielectric silica offered both thermal and structural stability. The enhancement, in this case, is mainly due to the increased Au NPs size [14]. The Tauc's curve in Fig. 6b further validated the previous result. There is no such difference obtained in the bandgap energy by using the $Au@SiO_2$ metal-dielectric core-shell.

Table 3
**Comparison of normalized absorption of PSCs with and without Au@ $SiO_2$ core-shell**

| Perovskite absorber layer | Values of normalized absorption of neat PSC (%) | Values of normalized absorption of PSC with core-shell (%) | Enhancement in normalized absorption (%) |
|---|---|---|---|
| Pure Perovskite | 76.84 | | |
| Pure $SiO_2$ | 76.42 | - | - |
| $Au@SiO_2$ (40nm) | - | 77.64 | 1.04 |
| $Au@SiO_2$ (30nm) | - | 78.90 | 2.6 |
| $Au@SiO_2$ (20nm) | - | 79.53 | 3.5 |

Moreover, the enhancement in the absorption with and without assuming $Au@SiO_2$ is shown in Table.3. The maximum enhancement of 3.5% was achieved in the overall optical absorption for $Au@SiO_2$ for $S_{tk}$ of 20nm. While in the other two cases for $S_{tk}$ of 30nm and 40nm, a very small enhancement was observed 1.04% and 2.6%, respectively.

# 5. Comparison Of Absorption Enhancement Of Au Nps, Au@tio 2, And Au@sio2 Core-shell

Finally, we compared all the simulated schemes embedded in the perovskite layer i.e., Au NPs, $Au@TiO_{2,}$ and $Au@SiO_2$ core shells. In the first scenario, we introduced monolayer and bilayer Au NPs embedded in the perovskite layer and investigated about 14.02% and 20.20% optical enhancement due to the LSPR effect, near field enhancement, and far-field scattering. In the second case, we introduced plasmonic Au NPs in pure $TiO_2$ to form core-shell nanostructure; the results are shown in Fig. 7a. a redshift, as well as enhancement in optical absorption, was observed by wisely incorporated Au NPs in $TiO_2$ nanoparticle to enhance the index of refraction of the insulting medium around the Au NPs. Because pure $TiO_2$ has the

capability to absorbed less than 5% of the solar spectrum [30]. We found the superior optical enhancement around 17.23% for embedding Au@$TiO_2$ core-shell in the perovskite layer is shown in Fig. 7a. Finally, in the case of incorporating Au@$SiO_2$ core-shell in the perovskite layer, a very slight redshift and very small 3.5% optical enhancement were observed in the absorption spectrum of PSC for the same $S_{tk}$ of 20 nm in both cases. The small increment in optical absorption is due to the low dielectric constant of silica as compared to the titania dielectric medium. Moreover, the reduced bandgap calculation from Tauc's curve also confirmed our previous outcomes. Similarly, the same concept was followed for the bandgap calculation of Au@$TiO_2$ core-shell and Au@$SiO_2$ core-shell. The decrease in bandgap achieved as the shell thickness decreases, for minimum shell thickness ($S_{tk}$ =20nm) of both Au@$TiO_2$ and Au@$SiO_2$ core-shell, the optimized reduced bandgap 1.52eV investigated as compared to pure perovskite.

# 6. Conclusion

In conclusion, we theoretically designed plasmonic and metal-dielectric core-shell nanostructure put in the active layer of PSCs and very wisely examined the plasmonics effect. Our optimized approach showed that the plasmonic effect strongly relies on the NPs size, shape, geometry, and the metal NPs and dielectric interaction. Firstly we have reported the enhancement in optical absorption of PSCs by inserting the Au NPs with different radii in the absorber layer due to the plasmonic effect. The Au NPs with increasing radii showed about 14% (g = 50nm) improved optical enhancement and achieved broad spectrum in PSCs as compared to neat PSCs without plasmonic effect. Secondly, we have also investigated the effect of $S_{tk}$ of Au@$TiO_2$ and Au@$SiO_2$ incorporated in the active perovskite layers and their influence on the optical absorption of PSCs. Our findings depicted that the $S_{tk}$ has a positive impact on the UV- Vis absorption of PSCs. The UV-Vis absorption increased as the size of the shell decreased. Finally, we compared the UV- Vis absorption of Au@$TiO_2$ and Au@$SiO_2$ for the same radii. The best optimum optical absorption is achieved in the case of Au@$TiO_2$ rather than in Au@$SiO_2$. The smart tailoring optical properties of Au NPs and their coupling with core-shell nanostructure open huge opportunities for future aspects to improve the technology in terms of chemical and thermal stability.

# Declarations

### Authors contribution

All authors systematically designed the conceptual study, developed the model and investigated the results. I.Ullah simulated the completed model from scratched and got the results. H. Saghaei and I.Ullah developed the methodology. I.Ullah has written the manuscript, H. Saghaei and S.K.Shah revised, edit and review the manuscript.

### Corresponding author

Ihsan Ullah

Institute of Functional Nano and Soft Materials, Soochow University, Suzhou 215123, China

Email: ehsankhan892@gmail.com

### Declarations

### Funding

The authors declare no funding recieived for this research work.

### Conflicts of interest

There are no conflicts to declare.

### Availability of data and materials

Not applicable

### Code Availability

Not applicable

### Availability of data and materials

Not applicable

### Ethics decalaration

### Ethics approval

Not applicable

### Consent to participate

Not applicable

## References

[1] A. Ecija, A. Larrañaga, K. Vidal, L. Ortega, and M. I. Arriortua, *Synthetic methods for perovskite materials; structure and morphology*: INTECH Open Access Publisher, 2012.

[2] N. K. Elumalai, M. A. Mahmud, D. Wang, and A. Uddin, "Perovskite solar cells: progress and advancements," *Energies,* vol. 9, p. 861, 2016.

[3] J. Huang, Y. Yuan, Y. Shao, and Y. Yan, "Understanding the physical properties of hybrid perovskites for photovoltaic applications," *Nature Reviews Materials,* vol. 2, pp. 1-19, 2017.

[4] M. A. Green, A. Ho-Baillie, and H. J. Snaith, "The emergence of perovskite solar cells," *Nature photonics,* vol. 8, pp. 506-514, 2014.

[5] S. A. Kandjani, S. Mirershadi, and A. Nikniaz, "Inorganic–organic perovskite solar cells," *Solar Cells-New Approaches and Reviews,* p. 450, 2015.

[6] A. Kojima, K. Teshima, Y. Shirai, and T. Miyasaka, "Organometal halide perovskites as visible-light sensitizers for photovoltaic cells," *Journal of the American Chemical Society,* vol. 131, pp. 6050-6051, 2009.

[7] H.-S. Kim, C.-R. Lee, J.-H. Im, K.-B. Lee, T. Moehl, A. Marchioro*, et al.*, "Lead iodide perovskite sensitized all-solid-state submicron thin film mesoscopic solar cell with efficiency exceeding 9%," *Scientific reports,* vol. 2, pp. 1-7, 2012.

[8] W. S. Yang, B.-W. Park, E. H. Jung, N. J. Jeon, Y. C. Kim, D. U. Lee*, et al.*, "Iodide management in formamidinium-lead-halide–based perovskite layers for efficient solar cells," *Science,* vol. 356, pp. 1376-1379, 2017.

[9] D. Liu, M. K. Gangishetty, and T. L. Kelly, "Effect of CH 3 NH 3 PbI 3 thickness on device efficiency in planar heterojunction perovskite solar cells," *Journal of Materials Chemistry A,* vol. 2, pp. 19873-19881, 2014.

[10] H. A. Atwater and A. Polman, "Plasmonics for improved photovoltaic devices," in *Materials for Sustainable Energy: A Collection of Peer-Reviewed Research and Review Articles from Nature Publishing Group*, ed: World Scientific, 2011, pp. 1-11.

[11] D. Derkacs, S. Lim, P. Matheu, W. Mar, and E. Yu, "Improved performance of amorphous silicon solar cells via scattering from surface plasmon polaritons in nearby metallic nanoparticles," *Applied Physics Letters,* vol. 89, p. 093103, 2006.

[12] M. D. Brown, T. Suteewong, R. S. S. Kumar, V. D'Innocenzo, A. Petrozza, M. M. Lee*, et al.*, "Plasmonic dye-sensitized solar cells using core– shell metal– insulator nanoparticles," *Nano letters,* vol. 11, pp. 438-445, 2011.

[13] I. Vangelidis, A. Theodosi, M. J. Beliatis, K. K. Gandhi, A. Laskarakis, P. Patsalas*, et al.*, "Plasmonic organic photovoltaics: unraveling plasmonic enhancement for realistic cell geometries," *Acs Photonics,* vol. 5, pp. 1440-1452, 2018.

[14] W. Zhang, M. Saliba, S. D. Stranks, Y. Sun, X. Shi, U. Wiesner*, et al.*, "Enhancement of perovskite-based solar cells employing core–shell metal nanoparticles," *Nano letters,* vol. 13, pp. 4505-4510, 2013.

[15] A. Furasova, E. Calabró, E. Lamanna, E. Tiguntseva, E. Ushakova, E. Ubyivovk*, et al.*, "Resonant silicon nanoparticles for enhanced light harvesting in halide perovskite solar cells," *Advanced Optical Materials,* vol. 6, p. 1800576, 2018.

[16] M. Batmunkh, T. Macdonald, W. Peveler, A. Bati, C. J. Carmalt, I. Parkin*, et al.*, "Plasmonic gold nanostars incorporated into high-efficiency perovskite solar cells," *ChemSusChem,* vol. 10, pp. 3750-3753, 2017.

[17] N. Aeineh, E. M. Barea, A. Behjat, N. Sharifi, and I. n. Mora-Seró, "Inorganic surface engineering to enhance perovskite solar cell efficiency," *ACS Applied Materials & Interfaces,* vol. 9, pp. 13181-13187, 2017.

[18] M. Sui, S. Kunwar, P. Pandey, and J. Lee, "Strongly confined localized surface plasmon resonance (LSPR) bands of Pt, AgPt, AgAuPt nanoparticles," *Scientific reports,* vol. 9, pp. 1-14, 2019.

[19] I. Khan, K. Saeed, and I. Khan, "Nanoparticles: Properties, applications and toxicities," *Arabian journal of chemistry,* vol. 12, pp. 908-931, 2019.

[20] P. B. Johnson and R.-W. Christy, "Optical constants of the noble metals," *Physical review B,* vol. 6, p. 4370, 1972.

[21] P. Löper, M. Stuckelberger, B. Niesen, J. Werner, M. Filipič, S.-J. Moon*, et al.*, "Complex Refractive Index Spectra of CH3NH3PbI3 Perovskite Thin Films Determined by Spectroscopic Ellipsometry and Spectrophotometry," *The journal of physical chemistry letters,* vol. 6, pp. 66-71, 2014.

[22] M. Filipič, P. Löper, B. Niesen, S. De Wolf, J. Krč, C. Ballif*, et al.*, "CH 3 NH 3 PbI 3 perovskite/silicon tandem solar cells: characterization based optical simulations," *Optics express,* vol. 23, pp. A263-A278, 2015.

[23] A. Hajjiah, I. Kandas, and N. Shehata, "Efficiency enhancement of perovskite solar cells with plasmonic nanoparticles: a simulation study," *Materials,* vol. 11, p. 1626, 2018.

[24] S. Roy and G. G. Botte, "Perovskite solar cell for photocatalytic water splitting with a TiO 2/Co-doped hematite electron transport bilayer," *RSC advances,* vol. 8, pp. 5388-5394, 2018.

[25] A. U. Rehman, M. Khan, A. D. Khan, J. Iqbal, M. Aslam, S. Khan*, et al.*, "Effect of plasmonic multilayered photoanode structures on the absorption of dye sensitized solar cell," *Japanese Journal of Applied Physics,* 2020.

[26] R. Fan, L. Wang, Y. Chen, G. Zheng, L. Li, Z. Li*, et al.*, "Tailored Au@ TiO 2 nanostructures for the plasmonic effect in planar perovskite solar cells," *Journal of Materials Chemistry A,* vol. 5, pp. 12034-12042, 2017.

[27] H. Lee, Y. K. Lee, E. Hwang, and J. Y. Park, "Enhanced surface plasmon effect of Ag/TiO2 nanodiodes on internal photoemission," *The Journal of Physical Chemistry C,* vol. 118, pp. 5650-5656, 2014.

[28] Z. Yuan, Z. Wu, S. Bai, Z. Xia, W. Xu, T. Song, *et al.*, "Hot-Electron Injection in a Sandwiched TiOx–Au–TiOx Structure for High-Performance Planar Perovskite Solar Cells," *Advanced Energy Materials,* vol. 5, p. 1500038, 2015.

[29] Y. Cheng, C. Chen, X. Chen, J. Jin, H. Li, H. Song, *et al.*, "Considerably enhanced perovskite solar cells via the introduction of metallic nanostructures," *Journal of Materials Chemistry A,* vol. 5, pp. 6515-6521, 2017.

[30] W. Li, A. Elzatahry, D. Aldhayan, and D. Zhao, "Core–shell structured titanium dioxide nanomaterials for solar energy utilization," *Chemical Society Reviews,* vol. 47, pp. 8203-8237, 2018.

# Figures

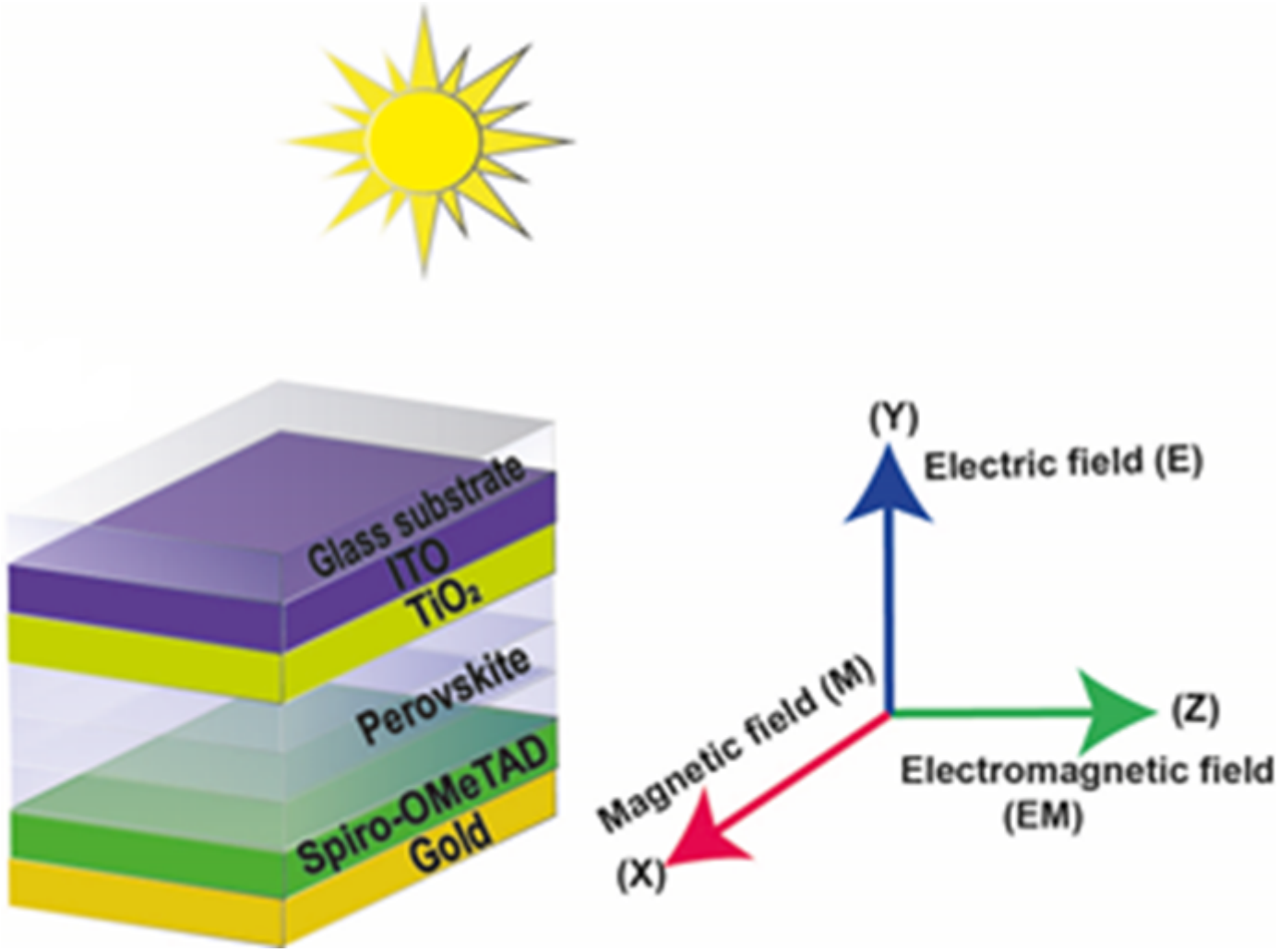


**Figure 1**

The Schematic of simple perovskite solar cell

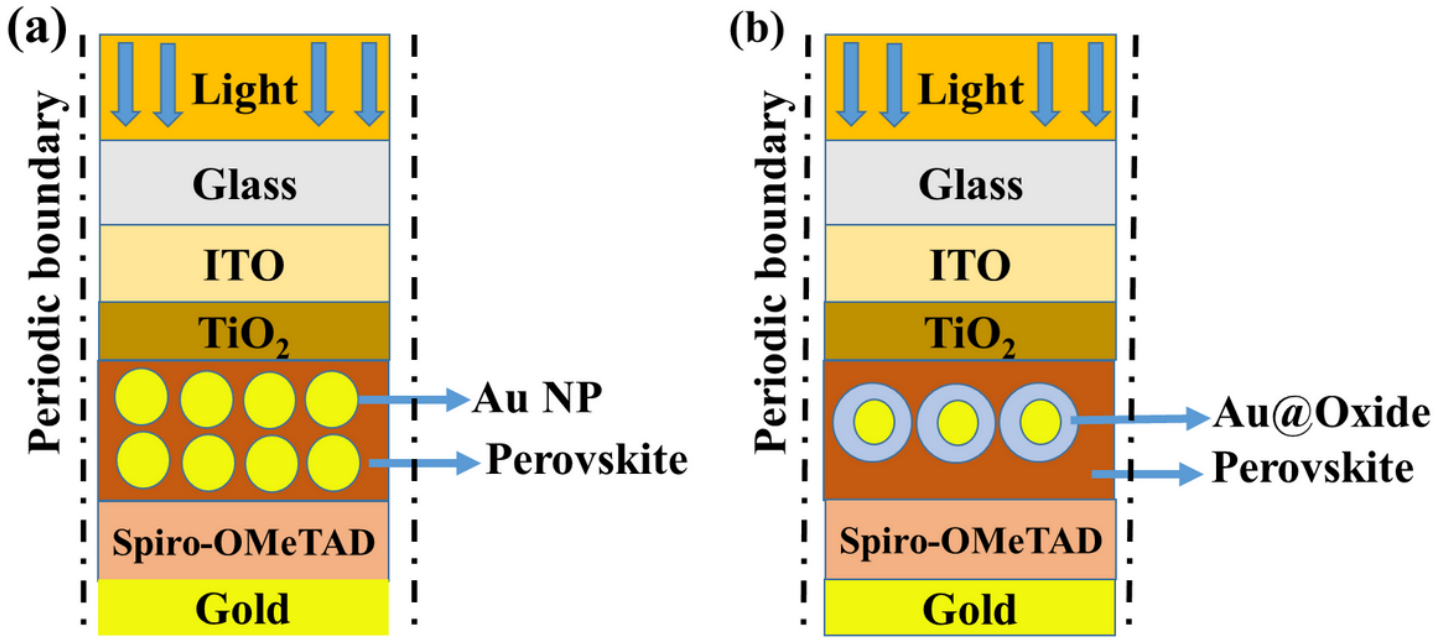


Figure 2

2-D Schematic. (a) Bilayer structure of Au NPs in perovskite layer (b) Core-shell structure in the perovskite layer.

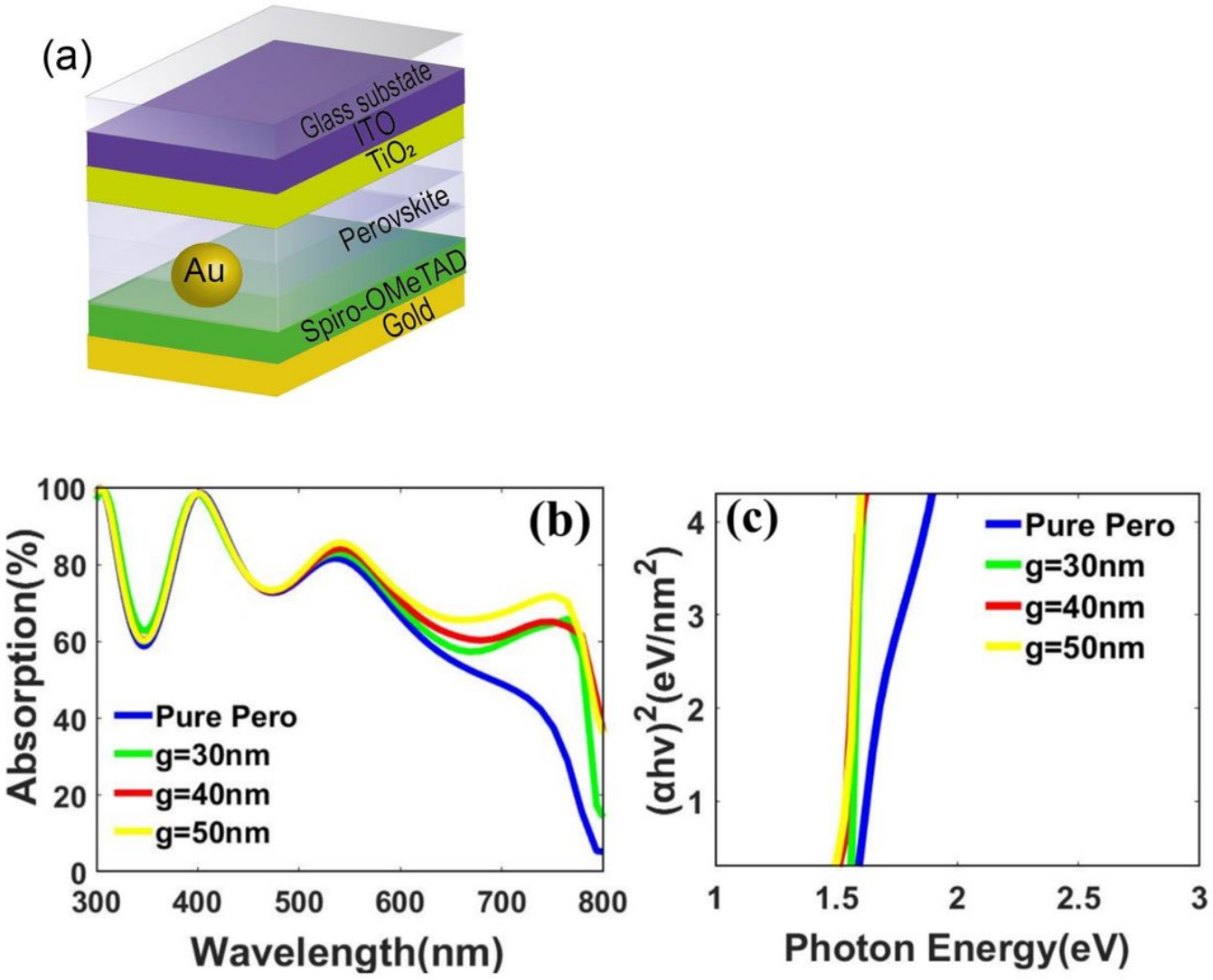


## Figure 3

The schematic of PSC (a) with monolayer Au NPs. Pure perovskite (blue line), perovskite with Au NPs (radius= 30, 40 and 50nm represented by green, red, and yellow color respectively) (b) The absorption spectra. (c) Tauc Curve

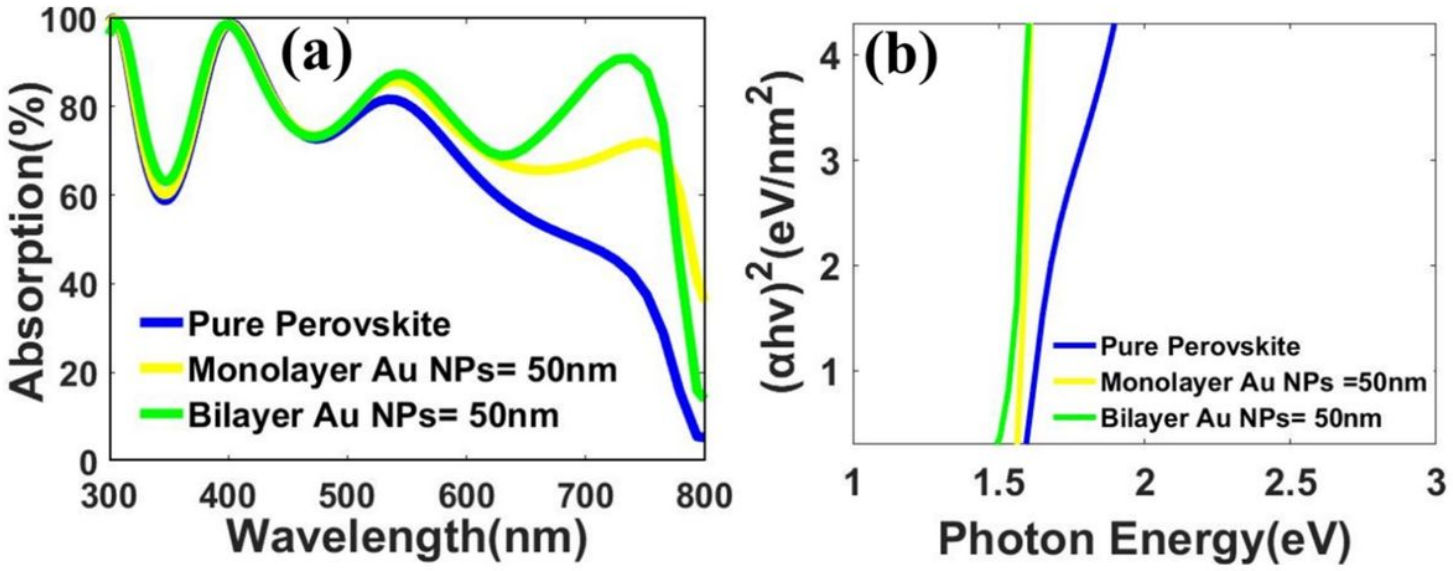


**Figure 4**

Comparison of UV-VIS absorption spectrum (a) W/O NP, monolayer NPs and bilayer NPs (b) Tauc's curve for bandgap

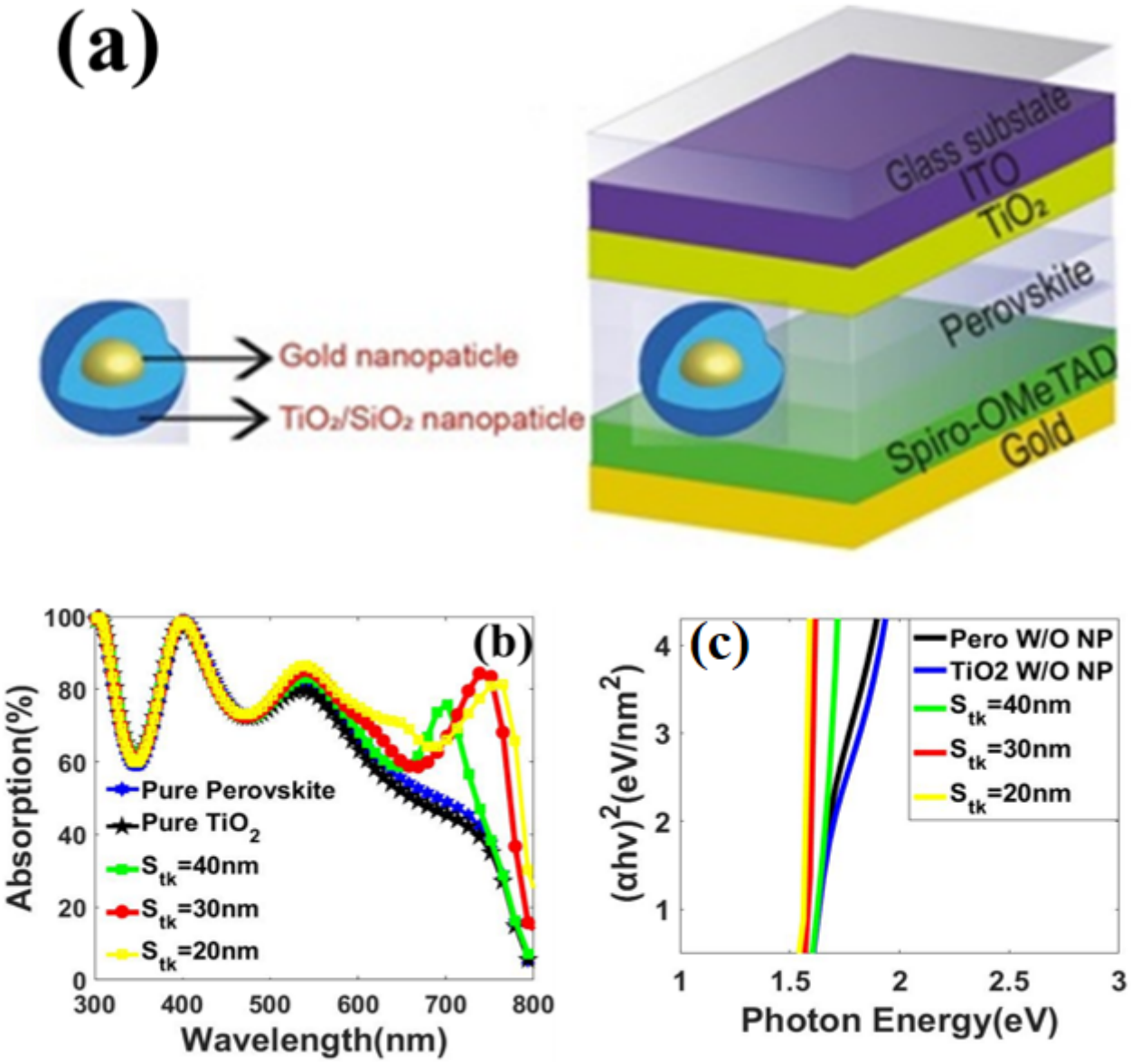


## Figure 5

Monolayer Au@TiO2 core-shell with thickness(Stk =40nm, 30nm, and 20nm) (a) 3-D Schematic of PSC with core-shell (b) UV-VIS spectrum (c) Tauc's curve for calculation of bandgap

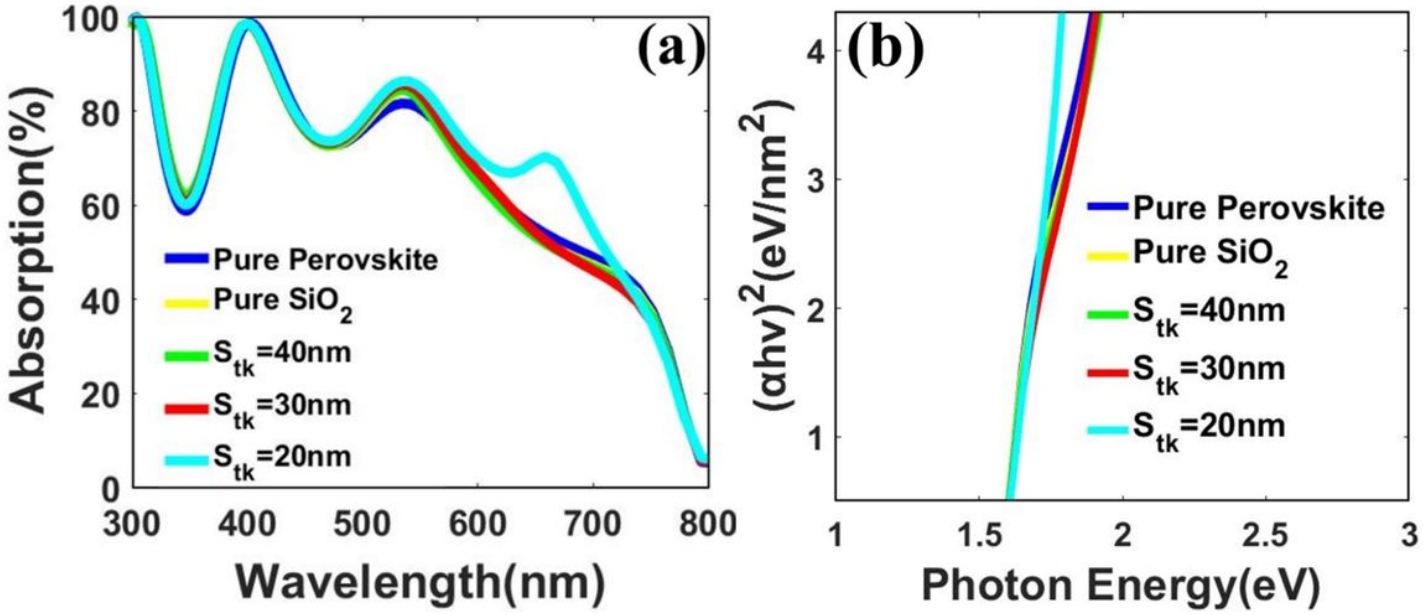


**Figure 6**

Monolayer Au@SiO2 core-shell with different sizes, i.e., 40nm. 30nm and 20nm (a) UV-VIS spectrum (b) Tauc's curve for bandgap calculations.

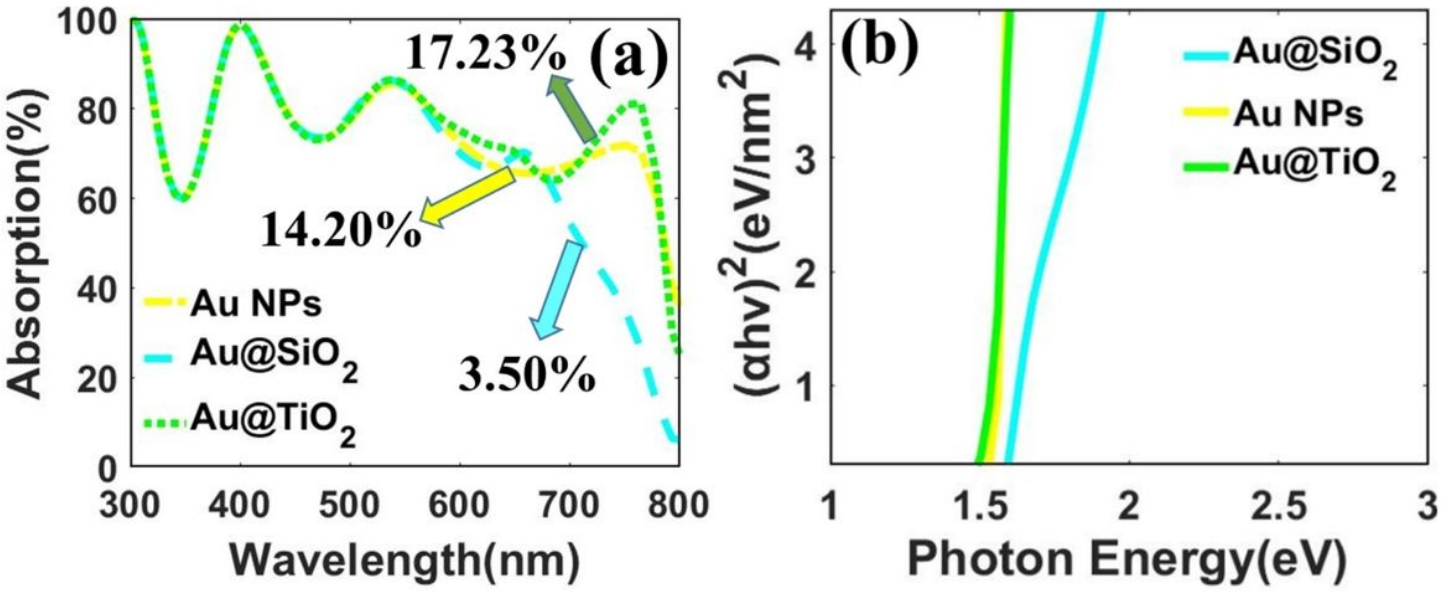


**Figure 7**

Comparison of all three different simulated schemes (a) Optical absorption spectrum of Au NPs (yellow color), Au@SiO2 (Blue color), and Au@TiO2 (green color) (b) Tauc's curve for Bandgap calculation.